Influence of Organic Modification on Mechanical Properties of Melt Processed Intercalated Poly(methyl methacrylate)–Organoclay Nanocomposites

Rajkiran R. Tiwari, Upendra Natarajan

Division of Polymer Science and Engineering, National Chemical Laboratory, Pune 411008, India

Received 30 September 2006; accepted 11 January 2007
DOI 10.1002/app.26192
Published online 26 April 2007 in Wiley InterScience (www.interscience.wiley.com).

ABSTRACT: The influence of organic modifiers on intercalation extent, structure, thermal and mechanical properties of poly(methyl methacrylate) (PMMA)–clay nanocomposites were studied. Two different organic modifiers with varying hydrophobicity (single tallow versus ditallow) were investigated. The nanocomposites were prepared from melt processing method and characterized using wide angle X-ray diffraction, transmission electron microscopy, thermogravimetric analysis, differential scanning calorimetry (DSC), and tensile tests. Mechanical properties such as tensile modulus (E), break stress (σ_{brk}), and % break strain (ε_{brk}) were determined for nanocomposites at various clay loadings. Extent of PMMA intercalation is sufficient and in the range 9–15 Å depending on organoclay and filler loading. Overall thermal stability of nanocomposites increases by 16–30°C. The enhancement in T_g of nanocomposite is merely by 2–4°C. With increase in clay loading, tensile modulus increases linearly while % break strain decreases. Break stress is found to increase till 4 wt % and further decreases at higher clay loadings. The overall improvement in thermal and mechanical properties was higher for the organoclay containing organic modifier with lower hydrophobicity and single tallow amine chemical structure. © 2007 Wiley Periodicals, Inc. J Appl Polym Sci 105: 2433–2443, 2007

Key words: nanocomposites; organoclay; structure; thermal properties; mechanical properties

INTRODUCTION

Polymer–clay nanocomposites have attracted researchers in the fields of polymers and material science with tremendous interest because of their unique physical and mechanical properties.[1] A great amount of research has been accomplished in this area where investigators have looked at many polymer hybrids with remarkable improvements in thermal properties,[2] better flame retardancy[2] and mechanical properties,[3] lower gas permeability,[4] among other property enhancements at low levels of clay loadings (typically <5% by wt) as compared to conventional microcomposites. There has been significant and growing interest in the study of nanocomposites with smectite type of silicate minerals, especially montmorillonite. Montmorillonite is generally preferred because of its lamellar structure which provides high stiffness and high aspect ratio (100–1000) accompanied by swellability and ease with which its surface can be chemically or physically modified. Montmorillonite bonding crystal structure consists of an octahedral alumina or magnesia sheet fused between two tetrahedral silica sheets, which form a single layer. Isomorphic substitution of ions within octahedral sheet (like Al^{3+} replaced by Si^{2+} or Mg^{2+}, Fe^{2+}, or Mg^{2+} replaced by Li^{+}) give rise to negative charge that is counterbalanced by alkali or alkaline earth cations (Na^{+}, Ca^{2+}, etc.) situated in the interlayer. Since the force that binds these layers is electrostatic in nature and is relatively weaker as compared to covalent bonding and therefore, Na^{+} or Ca^{2+} ions can be easily replaced by organic cations like alkylammonium ions by cation exchange procedure in solution. These organic alkylammonium cations lower the surface energy of clay and improve its wettability with typical non polar as well as mildly polar and dipolar polymers.

Atactic poly(methyl methacrylate) (PMMA) is an optically transparent material with good weatherability, high strength, scratch resistance, low water absorption, and stiffness.[5,6] PMMA–clay nanocomposites have been studied since last decade with most of the reports focusing on chemical synthesis route to hybrid preparation. PMMA–clay nanocomposites have been looked at using emulsion polymerization,[7] suspension polymerization,[8] solution polymerization,[8] and bulk polymerization[8,9] techniques. Exfoliated PMMA nanocomposites with various organoclays through emulsion polymerization technique[7] give

Correspondence to: U. Natarajan (u.natarajan@ncl.res.in).

improvement in thermal degradability. A comparitive study of structure, thermal, and mechanical properties of PMMA nanocomposites prepared using suspension, bulk, solution, and emulsion polymerization techniques by Wang et al.[8] has shown that either intercalated or exfoliated nanocomposites are formed depending on chemical nature of organic modifiers. For example, clay modified with fully aliphatic organic modifier results in intercalated nanocomposites, whereas the one containing double bond and allyl group can give either intercalated or exfoliated nanocomposites.[8] The tensile modulus is found to be higher for exfoliated nanocomposites as compared to intercalated ones,[8,9] whereas % elongation is known to be lower for nanocomposites in comparison with PMMA. Su and Wilkie[9] have shown that exfoliated PMMA nanocomposites can be formed at lower clay loadings ($\leq$0.5 wt %), whereas intercalated nanocomposites formed at higher clay loading ($\geq$3 wt %) from bulk polymerization of methyl methacrylate with *N*-methyl-*N*,*N* di(vinylbenzyl) octadecylammonium modified montmorillonite. Mechanical properties (Young's modulus and tensile strength) and onset of degradation are seen to be higher for nanocomposites as compared to PMMA.

At present relatively few reports exist on PMMA–clay nanocomposites using melt intercalation method[10–15] as compared to those prepared by other routes. Intercalated PMMA nanocomposites by melt blending PMMA with tetraallkyl ditallow ammonium modified bentonite[11] show improvement in thermal stability and T_g. Melt blended PMMA nanocomposites using polymerically modified organoclays show slight improvement in tensile properties for exfoliated PMMA nanocomposites at lower clay loadings till about 2.5 wt %.[12] Use of epoxy as dispersing agent of organomodified commercial nanoclay leads to exfoliated PMMA nanocomposites with improved mechanical properties.[13]

Our work here describes a detailed study on effect of organic modifier hydrophobicity on thermal and mechanical properties of PMMA–clay nanocomposites that are prepared by the melt processing method. Two different organoclays containing modifier having different polarity are studied. The main objective is to study the effect of organic modifier and its polarity on final properties of nanocomposites, as well as whether or not and in what manner polymer intercalation as a function of clay loading influences various mechanical properties. The clay dispersion and polymer intercalated was assessed using wide angle X-ray diffraction (WAXD) and transmission electron microscopy (TEM). The clay content in the nanocomposites was varied in the range 2–10% by weight. Results obtained for mechanical properties such as tensile modulus, tensile strength at break, and the % break strain are discussed.

EXPERIMENTAL

Materials and processing

Organically modified clays Cloisite® 20A and Cloisite® 25A (denoted henceforth C20A and C25A) were supplied by Southern Clay Products as a generous gift previously. Cloisite® 20A has dimethyl dihydrogenated-tallow quaternary ammonium (2M2HT) modifier with cation exchange capacity (CEC) of 95 mequiv/100 g. Cloisite® 25A has dimethyl hydrogenated-tallow 2-ethylhexyl quaternary ammonium (2MHTL8) organic modifier with CEC of 95 mequiv/100 g as organic modification. PMMA acrylpol-p 8015 used was supplied by Gujarat State Fertilizer, India. Melt flow index = 1.2 g/10 min (190°C/2.16 kg load) was determined using ASTM standard D1238. Molecular weights M_n = 50,865, M_w = 85,160, and PDI = 1.67 were determined by gel permeation chromatography technique using PMMA standard.

PMMA and organoclays used for nanocomposite preparation were dried at 65°C in an air circulatory oven for a period of 12 h prior to processing. PMMA and required amount of clay were dry mixed and melt blended at a temperature of 180°C in a HAAKE Rheocord mixer (capacity ~51 cm^3) at 60 rpm for mixing time of 10 min. PMMA nanocomposites have been prepared from melt compounding using processing temperature 175–200°C as seen in literature.[15] Processing temperature 180°C was chosen to avoid any significant thermal degradation of organic modifier, especially seen at higher temperatures from previous work and as known in literature. We determined that mixing speed of 60 rpm and mixing time period of 15 min gives maximum change in d_{001}-spacing with no change in level of intercalation with increasing mixing time for PMMA as well as other amorphous thermoplastic polymers like polystyrene (PS).

Nanocomposite characterization, measurements and property evaluation

Wide angle X-ray diffraction

WAXD patterns were recorded on a Rigaku (Japan) diffractometer with CuK_α radiation (wavelength λ = 1.5418 Å) at 40 kV and 100 mA. Experiments were performed in a scan range of $2\theta = 2°–14°$ with a scan speed of 2°/min and step size of 0.05 on compression-molded nanocomposite films. The films for WAXD analysis were prepared using compression molding in a carver press at 180°C for about 2 min at pressure of 5 MPa and cooled with water circula-

tion. Intercalation of PMMA in the clay interlayers spacing was confirmed by the shifts in d_{001} peaks from WAXD curves.

Transmission electron microscopy

Samples for TEM imaging were sectioned using a Lieca Ultracut UCT microtome. Sections of 50–70 nm thickness were obtained with a diamond knife at room temperature. Sections were collected from water on 300 mesh carbon coated copper grids. The copper grids were kept overnight on filter paper for drying. TEM imaging was done using a JEOL 1200EX electron microscope operating at an accelerating voltage of 80 kV. The density of clay particles is sufficient to produce contrast between polymer and clay stacks. Images were captured using charged couple detector camera and viewed using Gatan Digital Micrograph software.

Thermal analysis

Thermal measurements were carried on Perkin–Elmer DSC-7 differential scanning calorimeter (DSC). The DSC was calibrated using indium and sapphire as standards and nitrogen flow through DSC cell was maintained at 20 mL/min. Samples of approximately 5–10 mg were measured in an aluminum pan. Sample as well as reference chamber with an empty pan were heated at 10°C/min from 50 to 170°C to relieve any thermal history of the amorphous state. The sample was allowed to cool to 50°C at a rate of 50°C/min and subsequently reheated from 50 to 170°C. Heating was repeated at the same rate. The data obtained from the second scan was used to determine T_g of PMMA and nanocomposites. Thermogravimetric analysis (TGA) was performed using a Perkin–Elmer TGA-7. Samples of about 5–7 mg were heated from 50 to 700°C at a heating speed of 10°C/min, under nitrogen atmosphere (20 mL/min). Same heating rates were used for PMMA and the hybrid samples. Experiments were repeated on some samples to ensure accuracy of the results obtained.

Sample molding and mechanical testing

Specimens for tensile tests were prepared on a DSM-5 Micro-Compounder having an Injection molding machine attached to the compounder. The nanocomposites were melt using the micro-compounder at 190°C and 100 rpm for 5 min. The hybrid melt was then immediately injection molded with the barrel temperature set at 200°C and mold temperature at 35°C. Tensile tests were done on a 1 kN load cell at 27°C with a constant strain rate of 5 mm/min on Instron 4204 UTM machine. Tensile data were averaged over 10 independent measurements for each nanocomposite sample and system.

RESULTS AND DISCUSSION

Nanocomposite structure by WAXD and TEM analysis

WAXD is an accepted and most generally used method to determine either the formation of intercalated nanocomposites, or in a preliminary way the evidence of near complete exfoliation. d_{001}-spacing values and data for number of platelets per stack as calculated for intercalated PMMA nanocomposites are provided in Table I. Figures 1 and 2 show WAXD patterns of PMMA-C20A and PMMA-C25A nanocomposites at various clay loadings (range 2–10% by wt). d_{001} peaks for nanocomposites appear at lower 2θ angles as compared to peaks for organoclays, confirming increase in interlayer gallery spacing between clay layers due to the insertion of PMMA between successive layers as per Braggs law. As seen from Figure 1, the peak for Cloisite® 20A is at 2θ ~3.65° (d = 24.2 Å) whereas peaks for the corresponding nanocomposites are observed about 2θ approximately 2.5°–3.0°. Interlayer d_{001} peak for lower clay loadings (upto 4%) is relatively broader due to presence of some individual clay platelets as seen from WAXD curves and supported by the TEM pictures (Figs. 3 and 4). Also, there are no higher order peaks confirming complete intercalation of polymer uniformly within all silicate galleries, except at the high loading of 10% clay. The higher order peaks arising at higher clay loading has been previously observed for intercalated PMMA nanocomposites prepared using melt processing technique.[15]

At higher clay loadings (>4%) the d_{001} peak is quite sharp and of high intensities for nanocomposites of both types of structurally different organic

TABLE I
WAXD d_{001}-Spacings of Intercalated PMMA Nanocomposites

System	Clay (wt %)	d_{001}-spacing (Å)	Δd (Å)	No. platelets/stack
PMMA-C20A	2	33	8.8	3.2
PMMA-C20A	4	33	8.8	4.7
PMMA-C20A	6	33	8.8	4.8
PMMA-C20A	8	34	9.8	5.0
PMMA-C20A	10	35	10.8	5.5
PMMA-C25A	2	33	14.4	2.9
PMMA-C25A	4	33	14.4	3.6
PMMA-C25A	6	32	13.4	3.6
PMMA-C25A	8	33	14.4	4.0
PMMA-C25A	10	34	15.4	4.1

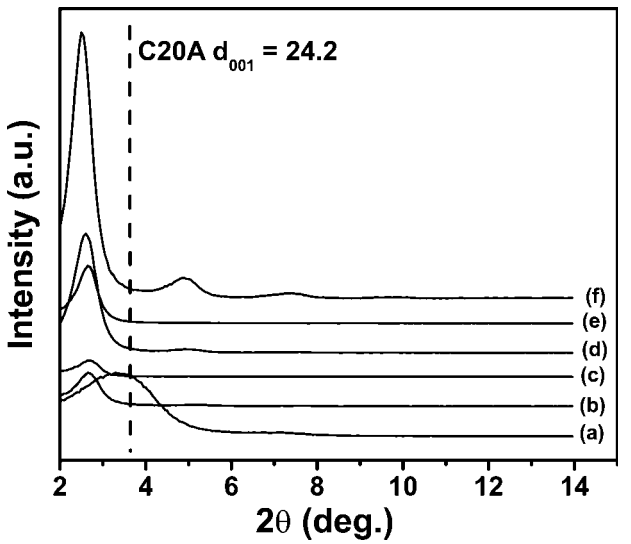

Figure 1 WAXD patterns for Cloisite® 20A (C20A) and PMMA nanocomposites: (a) Cloisite® 20A, (b) 2 wt % C20A, (c) 4 wt % C20A, (d) 6 wt % C20A, (e) 8 wt % C20A, and (f) 10 wt % C20A.

modifications (absolute values for Δd_{001} are provided in Table I). This shows that the morphology is strongly of intercalated type irrespective of the influence of the organic modifier. A second order peak, having *d*-spacing less than that of organoclays, appears at higher clay loadings for nanocomposites derived from either of the organic modifiers. At higher clay loading (10 wt %) relatively larger amount of clay is present in the matrix, some of which may remain unintercalated as a result of decrease in *d*-spacing resulting from compression of clay layers (*d*-spacings occur at smaller values as compared to the organoclay). This can occur due to some unavoidable degradation of the aliphatic quaternary ammonium organic modifier by shearing at the processing temperature used here. The effect of degradation during processing is more pronounced in the WAXD measurements at higher loadings. Moreover, the intensity of the primary intercalation peak increases at higher clay loading (10 wt %) confirming that the multilayer structure of intercalated clay is still preserved, which is also substantiated by TEM images (Figs. 3 and 4). These results essentially follow what is known in literature as regards influence of clay loading on nanocomposite phase structure behavior and d_{001}-spacings. We clearly observe uniformly consistent nanocomposite formation for loadings upto 8 wt % of the two types of chemically different organoclays.

The dispersion of clay particles within the matrix was determined by calculation of average number of clay layers forming tactoids using Scherrer equation,[16] as $L = (k\lambda)/(\beta_{001} \cos \theta)$ where L is average thickness clay stack, β_{001} (radian) is full width at half maximum for 001 reflection, and $k = 0.9$. The number of clay layers per stack (N) was calculated as $N = (L/d_{001}) + 1$. For PMMA nanocomposites, N was found to be 3–5.5. This indicates that the clay stacks consisting of 3–6 platelets are dispersed in the PMMA nanocomposites.

The amount of intercalated PMMA is more for Cloisite® 25A as compared to Cloisite® 20A systems. Cloisite® 20A, being more hydrophobic than Cloisite® 25A, provides a lower extent of thermodynamically favorable molecular interaction with PMMA as seen from d_{001}-spacing values in the present study as well as previous investigation.[15] Although the number of organic amine molecules per standard area of clay were similar for both clays (CEC being same for both clays 95 mequiv/100 g), Cloisite® 20A contains greater number of CH_2 groups per amine (dihydrogenated tallow) molecule as compared to Cloisite® 25A (single hydrogenated tallow).[15] This therefore reduces amount of favorable interaction between polymer segments and clay surfaces as well as between polymer segments and organic modifier segments in case of Cloisite® 20A as compared to Cloisite® 25A. We clearly observe (as shown in Table I) that extent of intercalation is not changing appreciably as a function of clay loading (±2 Å for the two organically modified PMMA nanocomposite systems) in the entire range (2–10 wt %). A near constancy of d_{001}-spacing shift with clay loading has been observed also for high molecular weight PS nanocomposites prepared with Cloisite10A organoclay, whereas for low and medium molecular weight PS the d_{001}-spacing has been found to decrease with clay loading and reach a plateau

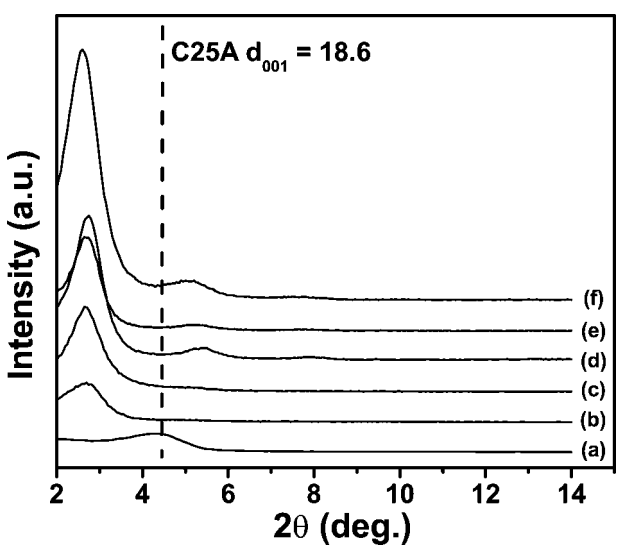

Figure 2 WAXD patterns for Cloisite® 25A (C25A) and PMMA nanocomposites: (a) Cloisite® 25A, (b) 2 wt % C25A, (c) 4 wt % C25A, (d) 6 wt % C25A, (e) 8 wt % C25A, and (f) 10 wt % C25A.

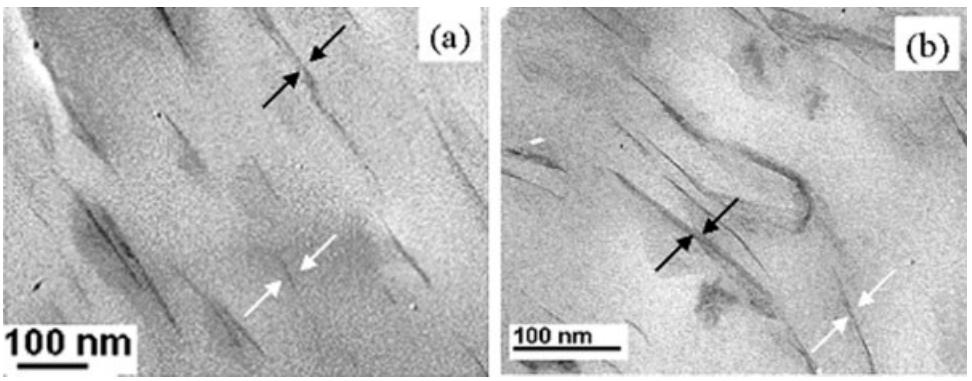

Figure 3 TEM images of PMMA nanocomposites at 2 wt % clay loading for (a) PMMA-C20A and (b) PMMA-C25A.

beyond 5 wt % of organoclay.[17] Tabtiang et al.[16] have also shown that in melt intercalated PMMA nanocomposites with dodecyl (C12) ammonium and hexadecyl (C16) ammonium modified clay, d_{001}-spacing does not change with clay content.

Bright field TEM images of PMMA nanocomposites, shown in Figures 3 and 4, were taken from injection molded samples and imaged in a direction normal to flow. Figure 3 shows the images for PMMA nanocomposites at 2 wt % clay loading. Dark lines represent silicate layers whereas bright region corresponds to PMMA. Figure 3(a,b) shows the intercalated clay layers along with some individual clay layers for PMMA-C20A and PMMA-C25A nanocomposites. Figure 4(a,b) shows TEM images at 10 wt % clay loading. An intercalated nanocomposite structure with regular and clearly aligned aggregates is obtained and confirms the result from WAXD measurements. The clay layers per stack are greater in number in nanocomposites at 10 wt % clay, which is also confirmed from relatively higher intensity peaks of WAXD pattern. More dispersible hybrids therefore are formed at lower clay loadings in contrast to those at higher loadings in both types of nanocomposites having different organic modifications.

Thermal properties of the hybrids

TGA overlays for PMMA and nanocomposites are shown in Figures 5 and 6. The nanocomposites show superior thermal degradation stability as compared to PMMA, mainly due to the presence of inorganic content in the form of lamellar intercalated structure that increases the stability of intercalated PMMA. TGA results for nanocomposites are shown in Table II; these include temperature values at 10% weight loss ($T_{10\%}$) that gives a relative measure of the onset of degradation, temperature at 50% weight loss ($T_{50\%}$), the weight % of residue (char) remaining at 700°C, and the maximum degradation temperature (T_{max}) as obtained from the differential DTG curve for each hybrid system. The data reveals that $T_{10\%}$ has gone up by a magnitude of 23°C for PMMA-C20A and 31°C for PMMA-C25A nanocomposite systems at 2 wt % clay loading. However, the stability is found to be less improved at 10% clay and this is a trend seen beyond 4% clay with increase in clay content. The improvement at low loadings is found to be as good as that at higher loadings and also comparable to that previously reported at higher loadings for PMMA-C25A system[15] (enhancement in $T_{5\%}$ by 26.5°C at 10 wt % clay).

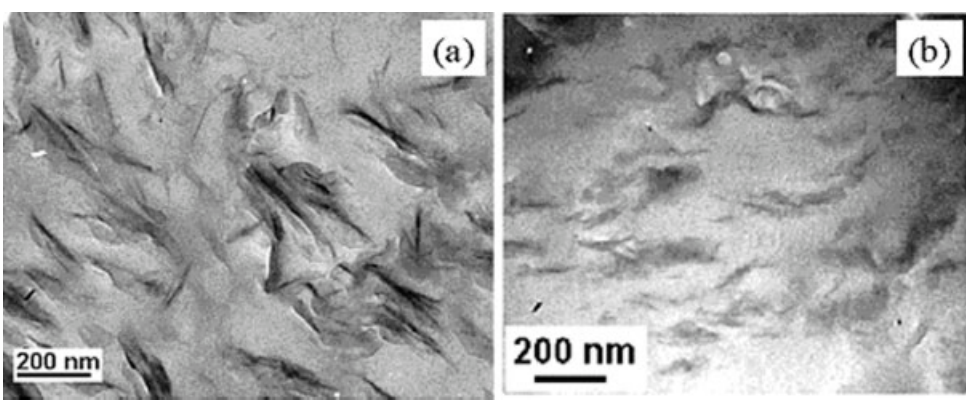

Figure 4 TEM images of PMMA nanocomposites at 10 wt % clay loading for (a) PMMA-C20A and (b) PMMA-C25A.

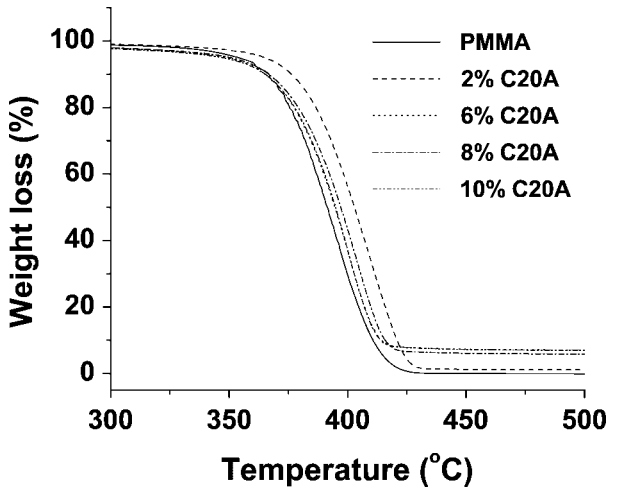

Figure 5 TGA thermographs of PMMA-C20A nanocomposites.

C20A organic modifier is more likely to undergo Hoffmann elimination reaction due to presence of ditallow, which has twice β-hydrogen sites compared to C25A. In such a case the thermal stability of C25A is higher than that of C20A. However, the degradation mechanism of organoclay in the presence of polymer chains is not well understood and needs further investigation. Xie at al.[18] have studied thermal degradation behavior of alkyl ammonium modified montmorillonite with varying alkyl chain length and have brought forth the 4-step degradation mechanism as compared to two-step degradation observed for unmodified clay. The onset of degradation for the bentonite (typically also for the southern clay organoclays) is found to be ~155°C. Further increase in temperature results in evolution of degradation products such as alkane, alkene, tertiary amine linear aldehyde, etc. The C20A modifier has higher probability to undergo Hoffmann elimination reaction as compared to C25A modifier due to presence of the ditallow aliphatic organic modifier. This explanation is supported by the thermal stability data of nanocomposites as seen from Table II. Similar degradation products are likely to be evolved for both organoclays studied here since their structures contain only aliphatic moeities.

TABLE II
TGA Data for PMMA and Its Nanocomposites at Different Loadings

System	Clay (wt %)	$T_{10\%}$ (°C)	$T_{50\%}$ (°C)	T_{max} (°C)	Char (%)
PMMA	0	353	380	386	0
PMMA-C20A	2	376	403	409	0.90
PMMA-C20A	4	373	401	409	2.75
PMMA-C20A	6	366	393	401	6.65
PMMA-C20A	8	367	397	405	5.50
PMMA-C20A	10	363	395	400	6.40
PMMA-C25A	2	384	411	417	1.25
PMMA-C25A	4	382	407	414	2.88
PMMA-C25A	6	377	403	409	4.55
PMMA-C25A	8	380	409	415	4.65
PMMA-C25A	10	378	407	413	7.00

Figure 7 shows DTG overlays at lower clay contents, which clearly shows the shift of main degradation peak towards higher temperature for nanocomposites resulting from improved thermal stability. Figure 8 presents the increase in maximum degradation temperature. The maximum increase in thermal stability occurs at lower clay loadings (till 4%), whereas at higher loadings it decreases. The maximum degradation temperature for PMMA-C25A systems is higher than for PMMA-C20A systems. This could also be due to more favorable interaction between PMMA and Cloisite® 25A as observed from the WAXD data (higher amount of intercalation and confined PMMA between clay layers). This greater confinement of PMMA between Cloisite®

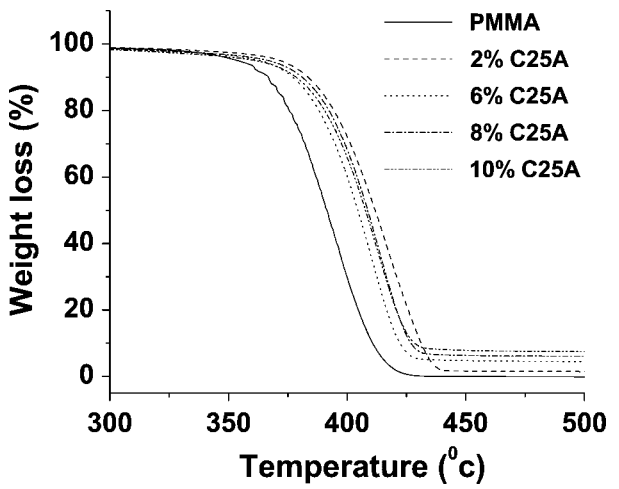

Figure 6 TGA thermographs of PMMA-C25A nanocomposites.

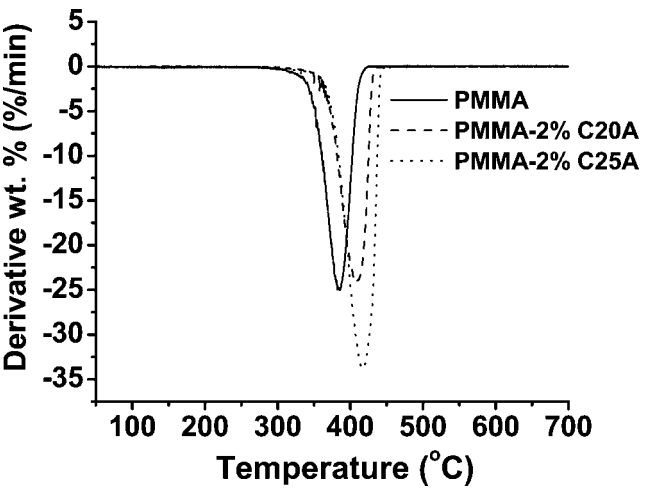

Figure 7 DTG overlay of PMMA and nanocomposites.

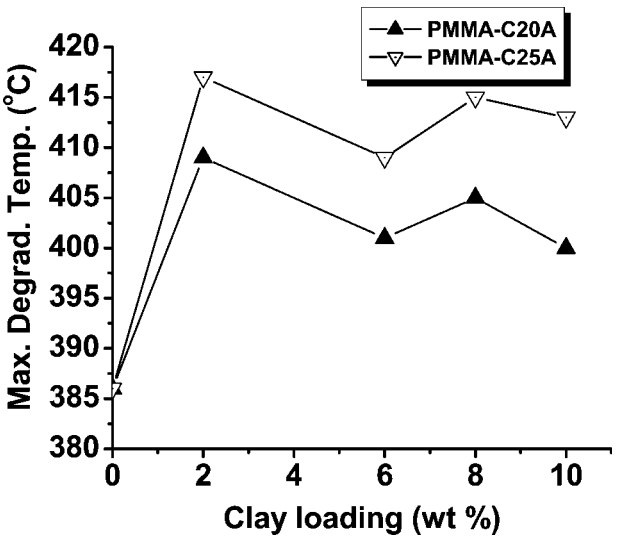

Figure 8 Variation of maximum degradation temperature of PMMA nanocomposites at various clay loadings.

25A layers as compared to Cloisite® 20A could also add to the better thermal stability of PMMA-C25A hybrids relative to PMMA-C20A hybrids. PMMA undergoes thermal degradation following β-scission at the chain ends giving rise to methyl methacrylate[19]; therefore, confined chains and chain-ends would relatively delay degradation response and diffusion of volatiles out of the hybrid. These results give some preliminary insight into how polymer–clay interactions and polymer–surfactant interactions control the physical properties of nanocomposites.

The effect of confinement of intercalated polymer on glass transition temperature and nondegradative thermal response was studied using DSC. Table III lists values of the T_g of PMMA–clay nanocomposites. The increase in T_g is shown consistently for both types of nanocomposites, which we feel is due to the effect of intercalation and the confinement of polymer segments. DSC curves for PMMA and its nanocomposites at various clay loadings with different organoclays are shown in Figures 9 and 10. PMMA shows T_g at 93°C; however, the intercalated system shows an increase in T_g by only upto 4°C over the range of clay loading and organoclay type studied here.

Contradictory effects are seen in literature for T_g of PMMA nanocomposites. Absence of T_g for PMMA nanocomposites prepared by emulsion polymerization has been observed.[20] The T_g of polymer–clay nanocomposites, as seen from literature, depends on preparation protocol/technique, chemical nature of organic modifier, amount of clay, mean dominant d_{001}-spacings of the interlayer gallery space, and the dispersion and arrangement of the clay stacks in the polymer matrix.[21] While a larger increase for intercalated hybrids as compared to exfoliated ones have been reported from melt blending method,[11] a lower T_g for intercalated hybrids as compared to unfilled matrix has also been observed for PMMA specifically.[15] Recently, Tabtiang et al.[16] have observed T_g for melt processed nanocomposites to be close to that of PMMA (therefore no significant change) and have attributed it to the unintercalated bulk polymer. Our present results over 2–10% clay range are in agreement with this recent observation.[16]

TABLE III
Glass Transition Temperatures of Intercalated PMMA Nanocomposite

System	Clay (wt %)	T_g (°C)
PMMA	0	93
PMMA-C20A	2	95
PMMA-C20A	4	94
PMMA-C20A	6	95
PMMA-C20A	8	96
PMMA-C20A	10	95
PMMA-C25A	2	94
PMMA-C25A	4	93
PMMA-C25A	6	97
PMMA-C25A	8	95
PMMA-C25A	10	96

Mechanical properties

Young's modulus

Mechanical properties such as Young's modulus (E), break stress (σ_{brk}), and the % break strain (ε_{brk}) were measured for PMMA nanocomposites. Variation of Young's modulus, break stress, and the % break strain as a function of clay loadings for these nano-

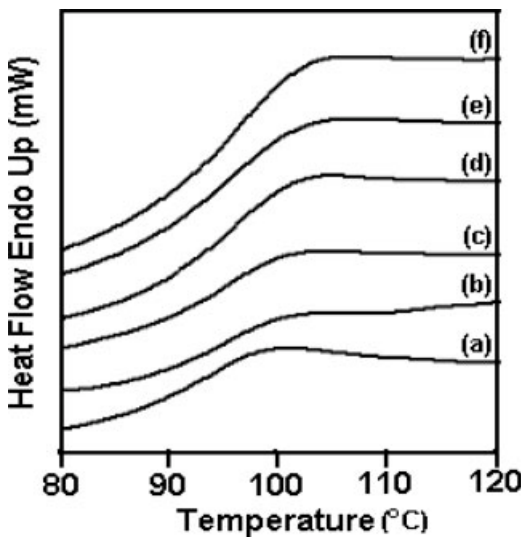

Figure 9 DSC thermographs of PMMA-C20A nanocomposites: (a) PMMA, (b) 2 wt % C20A, (c) 4 wt % C20A, (d) 6 wt % C20A, (e) 8 wt % C20A, and (f) 10 wt % C20A.

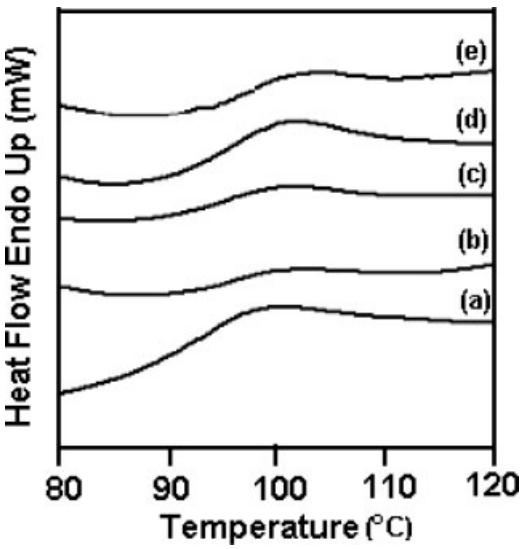

Figure 10 DSC thermographs of PMMA-C25A nanocomposites: (a) PMMA, (b) 2 wt % C25A, (c) 4 wt % C25A, (d) 6 wt % C25A, (e) 8 wt % C25A, and (f) 10 wt % C25A.

composites from the two different organically modified clays are shown in Figures 11–13. In the presence of organoclay in the Young's modulus of intercalated matrix shows significant improvement over that of PMMA. E increases from 6.8% to 57.0% and 13.4% to 68.9% with 2–10 wt % of clay for nanocomposites prepared with Cloisite® 20A and Cloisite® 25A, respectively. Tensile modulus increases linearly with clay fraction (correlation factor $r = 0.983$ and $r = 0.995$ for PMMA nanocomposites prepared with Cloisite® 20A and Cloisite® 25A). Such a linear

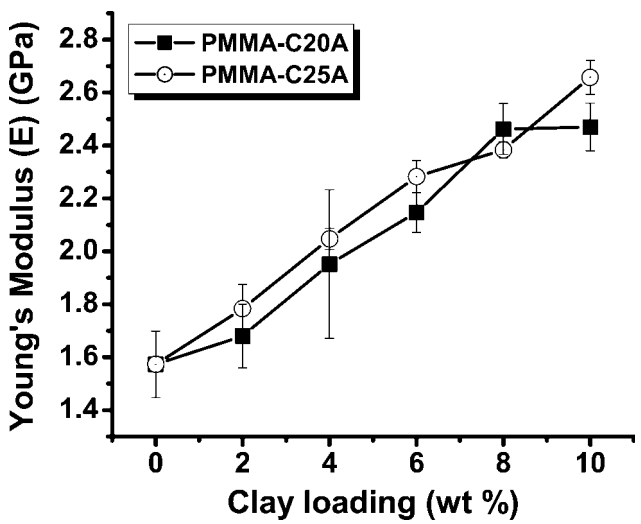

Figure 11 Variation of Young's modulus of PMMA nanocomposites with clay loading. The modulus of nanocomposites increases linearly with clay loading. The modulus for PMMA-C25A being higher than PMMA-C20A due to greater degree of favorable interaction between PMMA and C25A.

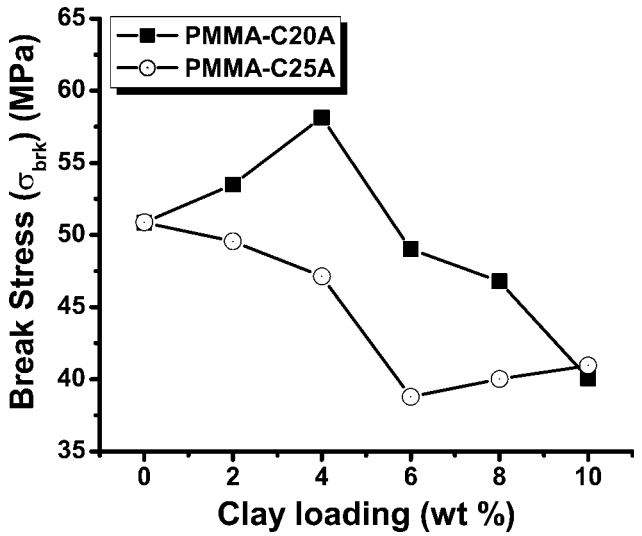

Figure 12 Variation of break stress of PMMA nanocomposites with clay loading.

increase has been observed previously for nanocomposites of various thermoplastic polymers such as SAN,[22] PS,[23] and polycarbonate.[24] The change in gallery height with clay loading, which is almost insignificant here, we find has no direct relationship with tensile modulus. However, effectively the total amount of confined polymer as determined by total amount intercalated (which scales as wt % clay) has a direct influence on modulus and other mechanical properties.

Tensile modulus is higher for nanocomposites prepared with Cloisite® 25A as compared to Cloisite® 20A, which is rationalized as follows. Although d_{001}-spacing of PMMA nanocomposites does not change significantly with clay loading, the amount of inter-

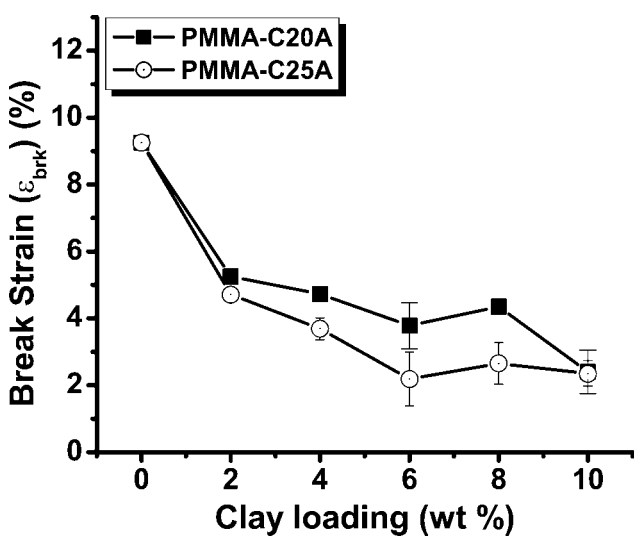

Figure 13 Variation of % elongation of PMMA nanocomposites with clay loading.

calated PMMA increases with loading at nearly fixed d_{001}-spacing. The amount of intercalated PMMA is greater in case of hybrids from Cloisite® 25A as compared to those from Cloisite® 20A as a result of more favorable interactions with former organoclay as discussed in the previous section. The Young's modulus as seen from some of the systems in literature such as for SAN nanocomposites is practically influenced by the aspect ratio of the filler in the matrix where higher aspect ratio increases interaction between polymer and clay surface and leads to higher modulus of nanocomposites (SAN nanocomposite data by Stretz et al.[22]). For nearly the same number of clay platelets per stack, as is the case here with PMMA nanocomposites at higher organoclay loading, the system having greater amount of intercalated polymer will give lower aspect ratio stack; however, this effect due to observed changes in d-spacings is not significant. The dominant effect is of higher level of confined polymer (Δd_{001}) and its interaction with clay (interlayer) that leads to higher modulus as seen for PMMA-C25A nanocomposites relative C20A hybrids. In comparison, the conventional composite prepared from PMMA and glass beads surface treated with γ-methacryloxy-propyltrimethoxysilane have also shown increase in modulus by 14% at 3 wt % of glass beads,[25] while we observe 30% increase at 4 wt % for intercalated Cloisite® 25A-PMMA system. Increase in modulus by 24 and 30.1% at 4 wt % of clay loading for nanocomposites prepared with Cloiste® 20A and Cloisite® 25A here are at similar levels as seen recently (32% at 3.8 wt % for intercalated PMMA nanocomposites prepared using methyl tallow bis-2-hydroxyethyl quaternary ammonium modified MMT by melt processing).[13]

Stretz et al.[22] have studied effect of various alkylammonium organic modifiers on tensile modulus of SAN nanocomposites and observed an increase in Young's modulus of nanocomposites prepared with clay containing lower molecular weight surfactants. Also, for SAN nanocomposites with organo-montmorillonite the polymer–clay interactions are more favorable in case of clay modified with quaternary ammonium of lower hydrophobicity (containing single C_{18} length typically). Similar trend is observed from our present study where montmorillonite modified with low molecular weight surfactant (Cloisite® 25A) gives higher Young's modulus than Cloisite® 20A that contains cationic surfactant of higher molecular weight. Observations on increase in modulus with clay loading have been made for PS[23] and PC.[24] For semicrystalline systems for example Fornes et al.[3] have looked at intercalated-exfoliated nanocomposites with nylon-6 using various organoclays with variation in amine content and exchange level relative to clay. Improvements by 66–71 and 30% for modulus and tensile strength for various organoclays at 4.6 wt % of montmorillonite are seen.[3] Chen et al.[26] have studied mechanical properties of MAH-g-PP-clay intercalated nanocomposite and observed increase up to 25 and 70% in tensile strength and tensile modulus resp. at 10 wt % of clay.

Tensile strength

As is known from literature the break stress of nanocomposites can either increase or decrease depending on nature of polymer, organic modifier in clay, and method of preparation.[8] The variation of tensile strength with clay loading is more complex than that of modulus and a clear understanding is still not established.[22] The break stress for PMMA-C25A is found to decrease with clay loading whereas it increases for PMMA-C20A nanocomposites till 4 wt % and further decreases at higher clay loadings. Therefore, at smaller levels of clay these different organic modifications have a different influence, while at higher than 4% the trends are uniform and similar with respect to clay loading. These nanocomposite samples were determined to be brittle at higher clay loadings as caused by significant reduction in break stress. At relatively high level of clay the break stress decreases by factor of 21.2 and 19.5% for nanocomposites from Cloisite® 20A and Cloisite® 25A, respectively, as compared to value of PMMA. Break stress is indicative of toughness of the material and it is generally not possible to maintain toughness along with modulus as has been shown for intercalated PMMA nanocomposites prepared by bulk polymerization route.[27]

Interestingly, here as shown by our data, the effect of organic modifier in case of break stress is opposite and different as compared to that observed for tensile modulus. Essentially the surfactant with higher molecular weight and relatively greater hydrophobicity (nos. of CH_2 groups) (Cloisite® 20A Mol. Wt. = 550) leads to a smaller change in intercalation Δd_{001} compared to surfactant with lower molecular weight and lower hydrophobicity (Cloisite® 25A Mol. Wt. = 410). Contrary to the behavior of the modulus, the break stress does not correlate positively with the level of intercalation, as we find that break stress is lower for nanocomposite with higher level of intercalation. For PMMA-C20A nanocomposites tensile strength decreases increases by 14% till 4 wt % clay and then reduces at higher loadings.

In comparison, melt processed intercalated PS nanocomposites[23] show increase in break stress at 2 wt % and further decrease at higher clay loading. For melt processed PC nanocomposites, break-stress data was not provided but the yield stress for

nanocomposites was found to be higher than that of polymer matrix.[24]

Break-strain

The decrease in ε_{brk} in intercalated amorphous thermoplastic nanocomposites[24] is attributed to brittleness incorporated by the clay particles in the polymer matrix. From our data for PMMA systems, ε_{brk} % is found to clearly decrease with increase in clay loading (by 74 and 75% for PMMA-C20A and PMMA-C25A at 10% clay). Therefore, upto 10 wt % clay in PMMA intercalated nanocomposites Δd_{001} (amount of polymer intercalation) does not have significant influence on ε_{brk}. A leveling of influence of clay % on ε_{brk} is observed beyond 6 wt %. Break-strain reduces by 48.8% and 60.1% at 4 wt % for PMMA-C20A and PMMA-C25A. Similarly, as seen from literature, melt processed intercalated PS nanocomposites[23] and polycarbonate nanocomposites[24] show decrease in elongational strain (at break) with increase in clay content.

The presence of filler creates a constrained environment for polymer chain mobility and reduces the elongation ability for intercalated nanocomposites. Increase in modulus and decrease in ε_{brk} has been consistently observed for thermoplastic nanocomposites.[8,27] Clearly, we establish here with our data that the effect of organic modifier on break stress and the % break strain is reverse than what is observed for the modulus. The decrease in break stress and break strain with increase in clay fraction in the matrix may be attributed to the brittle nature of the hybrids; however, no general systematic relationship has been observed on the effect of organic modifier on these properties till date for PMMA hybrids and even for other polymeric systems, conservatively *per se*. Further studies to understand the effect of chain length, primary versus secondary amine structure, and different organic modifiers of varying polarity, on structure and mechanical properties of PMMA-clay nanocomposites, are under investigation currently and would serve to expand understanding of such influences on properties.

CONCLUSIONS

Intercalated PMMA clay nanocomposites as prepared by melt processing were investigated to study the effect of organic modifier chemical structure on nanocomposite structure formation, thermal, and mechanical properties. WAXD results show the formation of intercalated nanocomposites, with broader peaks at lower clay loading resulting from partial exfoliation of clay layers in the polymer matrix. Thermal study showed increase in onset of degradation and an improvement in overall thermal stability. The T_g of nanocomposite is only slightly higher than that of the unfilled polymer. Tensile modulus for the nanocomposite with different organic modifications is found to increase linearly with clay loading, while the break strain is found to decrease. Break-stress for nanocomposites were lower than that of PMMA; however, a slight increase till 4 wt % followed by decrease at further increase in loadings was found for PMMA-C20A nanocomposites. The thermal properties and tensile modulus of nanocomposites are found to be higher for the clay containing aliphatic quaternary ammonium organic modifier with relatively lower hydrophobicity. We find clearly that relatively greater amount of intercalation drives better improvement in the tensile modulus of nanocomposites. This increase in modulus is directly related to an increase in amount of confined polymer within clay galleries and more favorable interactions with clay surface.

We thank the Council of Scientific and Industrial Research, India, for providing R.R.T. with the graduate Senior Research Fellowship. We are also thankful to Southern Clay Products, Inc., Texas, and appreciate the generous gift of the clay samples.

References

1. Ray, S. S.; Okamoto, M. Prog Polym Sci 2003, 28, 1539.
2. Zhu, J.; Morgan, A. B.; Lamelas, F. J.; Wilkie, C. A. Chem Mater 2001, 13, 3774.
3. Fornes, T. D.; Yoon, P. J.; Hunter, D. L.; Keskkula, H.; Paul, D. R. Polymer 2002, 43, 5915.
4. Yano, K.; Usuki, A.; Okada, A. J Polym Sci Part A: Polym Chem 1997, 35, 2289.
5. Brandrup, J.; Immergut, E. H. Polymer Handbook, 3rd ed.; Wiley Interscience: New York, 1989.
6. Li, Y.; Zhao, B.; Xie, S.; Zhang, S. Polym Int 2003, 52, 892.
7. Zheng, J. P.; Wang, J. X.; Gao, S.; Yao, K. D. J Mater Sci 2005, 40, 4687.
8. Wang, D.; Zhu, J.; Yao, Q.; Wilkie, C. A. Chem Mater 2002, 14, 3837.
9. Su, S.; Wilkie, C. A. J Polym Sci Part A: Polym Chem 2003, 41, 1124.
10. Salahuddin, N.; Shehata, M. Polymer 2001, 42, 8379.
11. Shen, Z.; Simon, G. P.; Cheng, Y. J Appl Polym Sci 2004, 92, 2101.
12. Su, S.; Jiang, D. D.; Wilkie, C. A. Polym Degrad Stab 2004, 83, 321.
13. Park, J. H.; Jana, S. C. Polymer 2003, 44, 2091.
14. Kim, Y.; White, J. L. J Appl Polym Sci 2005, 96, 1888.
15. Kumar, S.; Jog, J. P.; Natarajan, U. J Appl Polym Sci 2003, 89, 1186.
16. Tabtiang, A., Kumlong, S., Venables, R. A. Eur Polym J 2000, 36, 2559.
17. Tanoue, S.; Utracki, L. A.; Rejon, A. R.; Tatibouët, J.; Kenneth, C. C.; Kamal, M. R. Polym Eng Sci 2004, 44, 1046.
18. Xie, W.; Gao, Z.; Pan, W. P.; Hunter, D.; Singh, A.; Vaia, R. A. Chem Mater 2001, 13, 2979.
19. Jang, B. M.; Costache, M.; Wilkie, C. A. Polymer 2005, 46, 10687.

20. Lee, D. C.; Jang, L. W. J Appl Polym Sci 1996, 61, 1117.
21. Yeh, Y. M.; Liou, S. J.; Lai, M. C.; Chang, Y. W.; Huang, C. Y.; Chen, C. P.; Jaw, J. H.; Tsai, T. Y.; Yu, Y. H. J Appl Polym Sci 2004, 94, 1936.
22. Stretz, H. A.; Paul, D. R.; Li, R.; Keskkula, H.; Cassidy, P. E. Polymer 2005, 46, 2621.
23. Tanoue, S.; Utracki, L. A.; Rejon, A. R.; Tatibouët, J.; Kamal, M. R. Polym Eng Sci 2005, 45, 827.
24. Yoon, P. J.; Hunter, D. L.; Paul, D. R. Polymer 2003, 44, 5323.
25. Maspoch, M. L.; Tafzi, A.; Ferrando, H. E.; Velasco, J. J.; Benasat, A. M. Macromol Symp 2001, 169, 159.
26. Chen, L.; Wong, S. C.; Pisharath, S. J Appl Polym Sci 2003, 88, 3298.
27. Qu, X.; Guan, T. G.; Liu, G.; She, Q.; Zhang, L. J Appl Polym Sci 2005, 97, 348.